Proceedings of the 28th IEEE
EMBS Annual International Conference
New York City, USA, Aug 30-Sept 3, 2006

Extraction and Tracking of MRI Tagging Sheets Using a 3D Gabor Filter Bank

Zhen Qian, Dimitris N Metaxas and Leon Axel

Abstract— **In this paper, we present a novel method for automatically extracting the tagging sheets in tagged cardiac MR images, and tracking their displacement during the heart cycle, using a tunable 3D Gabor filter bank. Tagged MRI is a non-invasive technique for the study of myocardial deformation. We design the 3D Gabor filter bank based on the geometric characteristics of the tagging sheets. The tunable parameters of the Gabor filter bank are used to adapt to the myocardium deformation. The whole 3D image dataset is convolved with each Gabor filter in the filter bank, in the Fourier domain. Then we impose a set of deformable meshes onto the extracted tagging sheets and track them over time. Dynamic estimation of the filter parameters and the mesh internal smoothness are used to help the tracking. Some very encouraging results are shown.**

I. Introduction

Tagged cardiac magnetic resonance imaging is a well-known technique for non-invasively visualizing the detailed myocardial motion and deformation. It has the potential of early diagnosis and analysis of cardiovascular disease. This technique generates a set of parallel tagging planes within the myocardium as temporary markers at end-diastole by spatial modulation of magnetization. As in Figure 1, the imaging planes are perpendicular to the tagging planes, so that the tagging planes appear as a set of parallel dark stripes in the MR images and deform with the underlying myocardium during the cardiac cycle *in vivo*. This provides the motion information of the myocardium in the normal direction of the tagging stripes. However, finding an efficient and robust method to automatically extract and segment out these tags and track their deformation over time is still a challenging task. Based on the spatial and frequency characteristics of the tag pattern, several researchers have employed different Fourier-based filtering methods to this problem, such as HARP [1], [2], which is basically a band pass filter; and a 2D Gabor Filter bank [3], [4], which is a set of 2D Gabor filters with a bank of tunable parameters that represent the variant spacing and orientation of the tagging lines. Gabor filtering achieves optimal localization in both the spatial and the frequency domains, which makes it more suitable for the tag analysis. In [3] a method that combined each filter's response in a filter bank and segmented the 2D tagging lines was presented. By finding optimal parameters that maximize the Gabor filter response at each location in the MR image, researchers in [4] extracted deformation and motion information in a 2D simulated model. However, these 2D approaches have limitations. They track the tagging lines' displacement only in a single spatial slice, while the tagging lines are actually the intersections of the tagging sheets and the imaging planes. Thus observation of the 3D tagging sheet deformation is more desirable in heart wall motion modeling and analysis. Because of the shearing and out of image-plane motions of the heart wall, the initial tagging planes are no longer true planes but turn to curved, bend or even twisted tagging sheets. Finding the tagging lines' correspondence across the imaging slices, i.e., which set of tagging lines belong to the same tagging sheet, is essential to recovering the deformed tagging sheets. A 3D tracking approach is necessary in finding this tagging line correspondence.

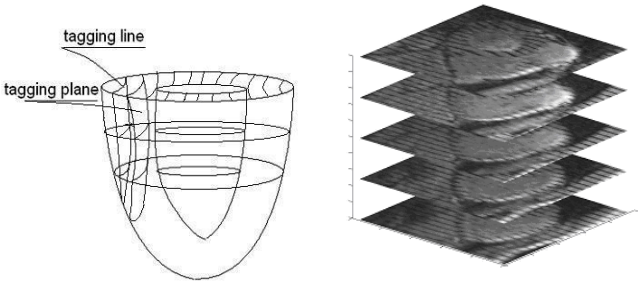

(a) (b)

Fig. 1. (a) shows tagging lines are intersections of the tagging sheets and the imaging planes. (b) shows a 3D tagged MR image dataset.

In this paper, we extend our 2-D Gabor filter bank method [3], [4] to employ a 3-D Gabor filter bank in order to extract and track the deformed tagging sheets. The filter's scale, orientation, and shape are specified according to the geometric pattern of the tagging sheets. We convolve the 3D Gabor filter bank with the 3D tagged MRI data, which are in a time sequence. For each set of the 3D data, we extract the tagging sheets by combining the strong outputs from the filter bank at each voxel. Then we impose a deformable 3D mesh onto each of the tagging sheet to capture the tagging sheet deformation. In the following section, we first outline our theory and then some promising experiment results are presented.

II. Basic Definitions: 3-D Gabor filter

The 1-D Gabor filter was first introduced by D. Gabor in 1946 [5]. It is basically a product of a Gaussian window and a complex sinusoid. 3-D Gabor filter is a 3D extension of its 1-D form and has been used in many image processing and

Zhen Qian and Dimitris N Metaxas are with the Department of Biomedical Engineering, Rutgers University, Piscataway, NJ 08854, USA zqian@eden.rutgers.edu, dnm@cs.rutgers.edu

Leon Axel is with the Department of Radiology, New York University, New York, NY 10016, USA Leon.Axel@nyumc.org

computer vision fields, such as 3-D texture segmentation [6], [7], [8], motion analysis [9], and object recognition [10]. If we extend the 1-D function to 3-D, we get

$$h(x,y,z) = g(x',y',z') \cdot s(x,y,z) \tag{1}$$

where $g(x',y',z')$ is a 3-D Gaussian envelope, and $s(x,y,z)$ is a complex sinusoid function, i.e.,

$$g(x',y',z') = \frac{1}{(2\pi)^{\frac{3}{2}}\sigma_{x'}\sigma_{y'}\sigma_{z'}} e^{-\frac{1}{2}[(\frac{x'}{\sigma_{x'}})^2+(\frac{y'}{\sigma_{y'}})^2+(\frac{z'}{\sigma_{z'}})^2]} \tag{2}$$

$$s(x,y,z) = \exp[-j2\pi(Ux+Vy+Wz)] \tag{3}$$

In Equation 2: $(x',y',z')^T = R \times (x,y,z)^T$ are the rotated spatial coordinates of the Gaussian envelope. R is a rotation matrix. Note that $\sigma_{x'}$, $\sigma_{y'}$ and $\sigma_{z'}$ may not be the same. Thus the shape of this Gaussian envelope can be an ellipsoid. In Equation 3, (x,y,z) is non-rotated spatial coordinates, which means the Gaussian envelope and the sinusoid could have different orientations. However, for normalization purposes. We set these two coordinates to the same value. (U,V,W) are the 3D frequencies of the complex sinusoid. They determine a Gabor filter's orientation and spacing in the spatial domain. As shown in Fig 2, a 3D Gabor filter has sets of iso-surfaces such that all those voxels on the same iso-surface have a constant value, for instance, in Fig 2(a), all the same colored voxels are on a same set of iso-surfaces; in Fig 2(b), one set of the iso-surfaces is drawn as the yellow pancakes. The parallel iso-surfaces are geometrically similar with the 3D MR tagging sheets in the local regions. This makes it suitable for tagging sheet extraction and segmentation. The normal of these iso-surfaces is a constant and set by:

$$\vec{N}_{isosurface} = (U,V,W) \tag{4}$$

At the same time, the spacing between two neighboring iso-surfaces is also a constant and set by:

$$S_{isosurface} = \frac{1}{\sqrt{U^2+V^2+W^2}} \tag{5}$$

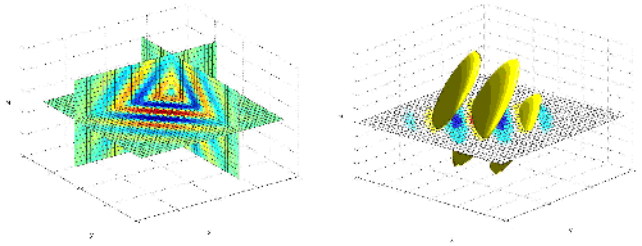

(a) (b)

Fig. 2. (a) A slice view of a 3D Gabor filter. (b) An iso-surface view of a 3D Gabor filter. Here $\sigma_{x'} = \sigma_{y'} = \sigma_{z'}$, which makes the Gaussian envelope symmetric and the iso-surfaces in (b) circle-shaped; the normal of these iso-surfaces are (1,1,1), because $U = V = W$.

III. Methodology

A. 3D Gabor filters design

Tagging sheets are initialized and appear as a set of parallel and equally spaced dark planes in the myocardium at the end of diastole. During systole, tagging sheets deform with the underlying heart tissue so that the spacing and orientation of these tag sheets change over time. For short axis (SA) cardiac MR images, for instance, see Figure 3(a), a tag sheet T is initially perpendicular to the imaging plane I. For T, there are three possible rotation angles, ϕ, ψ, and φ with respect to the three rotation axes. φ is the rotation angle w.r.t. the axis that is perpendicular to the tagging sheets. Thus φ measures the in-tagging-sheet rotation, which is not observable from the motion of the tagging sheet. So for SA images, we only consider the other two possible rotation angles: ϕ is the rotation angle w.r.t. the z axis, and ψ is for the rotation w.r.t. the intersection line of the tagging sheet and the imaging plane.

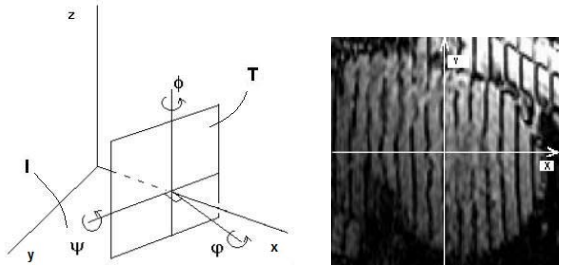

(a) (b)

Fig. 3. (a) Tagging sheet's rotation has three possible orientations. But only ϕ, ψ are observable. The in-plane rotation φ is ignored. (b) The y axis is set to parallel to the initial tagging lines.

Since the initial tagging planes are perpendicular to the imaging planes, we set the $x-y$ plane parallel to the imaging planes, i.e., the 2D image slices. In the $x-y$ coordinates, we rotate the 2D image so that the y axis is parallel to the initial tagging lines. See Figure 3(b).

In Equation 3, the Gabor sinusoid is specified by (U,V,W). However, when we design the Gabor filter to extract the tagging sheets, we are more interested in certain meaningful parameters, such as the spacing S between the tagging sheets, and the sheets' observable orientations ϕ and ψ. Actually from Equation 4 and 5, we are able to use S, ϕ, and ψ to represent (U,V,W):

$$V = \frac{S}{\sqrt{(1+\tan^2(\phi)) \cdot (1+\tan^2(\psi))}} \tag{6}$$

$$U = V \cdot \tan(\phi) \tag{7}$$

$$W = \tan(\psi) \cdot \sqrt{U^2+V^2} \tag{8}$$

In Equation 2, we use an ellipsoid-shaped 3D Gaussian envelope, which is more adaptable to the myocardial geometries and the tag patterns. The long axis of the 3D Gaussian is set to the same as the x axis so that it can cover more tag

patterns. We experimentally define the σ's in Equation 2 as follows.

$$\sigma_x = \frac{1}{S}, \sigma_y = \frac{1}{4S}, \sigma_z = \frac{1}{4S} \quad (9)$$

The rotation matrix of the Gaussian envelope is given by:

$$R = R_z \times R_{xy} = \begin{bmatrix} 1 & 0 & 0 \\ 0 & cos(\phi) & -sin(\phi) \\ 0 & sin(\phi) & cos(\phi) \end{bmatrix} \times \begin{bmatrix} cos(\psi) & -sin(\psi) & 0 \\ sin(\psi) & cos(\psi) & 0 \\ 0 & 0 & 1 \end{bmatrix} \quad (10)$$

This rotation step is to make the Gaussian envelope have the same orientation as the complex sinusoid, which is important for the normalization purpose.

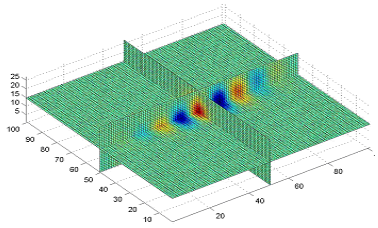

Fig. 4. A Slice view of a 3D Gabor Filter used in our experiment.

B. Interpolation and Parameter Tuning

Usually, the 3D MRI data have different sampling rates in each coordinate. For instance, in our dataset, in the x and y coordinates, the pixel size equals 1.3 mm, while in the z coordinate, the spacing between two neighboring slices is 5.2 mm. This means the in-plane sampling rate is about 3 times higher than the inter-plane rate. To solve this discrepancy, we consider our 3D image as a set of data that is contracted by 4 times in the z direction. Thus contraction in the spatial domain will lead to an expansion in the Fourier domain. We set the new $W' = W \times 4$, which represents that the frequency in z direction is expanded by 4 times. And at the same time, the Gaussian envelope is also contracted in the z direction. We set the new $\sigma'_z = \sigma_z/4$ and the new $\psi' = arctan(\tan(\psi) \times 4)$, which is the new rotation angle for the Gaussian. See Figure 4 for an example of the Gabor filter in our case.

The tunable parameters of the 3D Gabor filter bank are ϕ, ψ and S. The initial ϕ_0 and S_0 are obtained by solving the inverse of the Equations 6 and 7. The (U, V) are obtained by finding the frequencies of the fundamental harmonic of a 2D image slice at the beginning of the systole from the 3D dataset [3]. The initial ψ_0 is set to zero, since the initial tagging sheets are perpendicular to the imaging plane. In our experiments, we modulate the parameters ϕ, ψ and S based on the possible deformations of the myocardium. For example, the spacing between two tagging sheets may likely increase to double width or decrease to half width during myocardial deformation, thus we tune S so that $S_0/2 \leq S \leq 2S_0$. The bank of Gabor filters is made up of all possible filters whose parameters are in the tuning range.

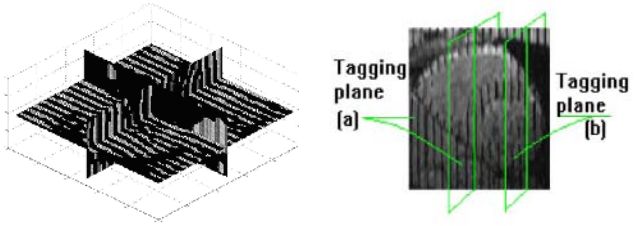

(a) (b)

Fig. 5. a) A slice view of the 3D Segmentation result. b) The two tagging sheets that are tracked along time sequences. Tracking results of the sheets are shown in Fig 7.

IV. Experimental Details and Results

We tried our method on four 4D datasets, whose resolution are 96x96x18 pixels and consist of 6 time sequences, i.e., each dataset contains 108 2D images. All our experiments were coded in Matlab on a P4 1.5G desktop computer. The analysis of each dataset took approximately 15mins. Figure 5(a) shows an extraction result at time 6. This result is a combination of all the responses of the Gabor filter bank. The combination and normalization method is as follows: we assume that using Gabor filters, the total number of voxels within the tag sheets is a constant. First, this total number is estimated in an initialization step. Then using different Gabor filters, we pick out for each filter the 90% number of pixels with the highest values. The final result is a combination of all the results from each Gabor filter. As shown in Figure 5(a) it is a binary image cube where the extracted tagging sheets have the value of one and the else places are zero.

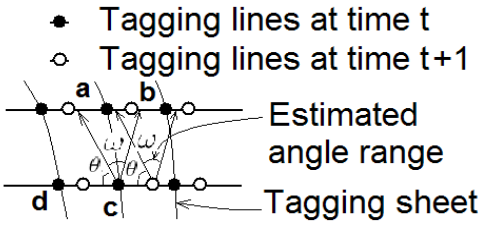

Fig. 6. The rotation angle ψ at time $t+1$ is constrained by the angle ω and θ at time t, which prevents tagging sheets aliasing.

The binary image does not give the tagging lines' correspondences across the image slices. In the tracking step, we impose a set of deformable meshes onto the initial tagging planes and let them deform according to the extracted tagging sheet results over time. The above binary image cube gives the possible locations where the tagging sheets may move to. And as in Figure 6, the range of ψ at time $t+1$ is constrained by the angle ω and θ, which equal $\angle acb$ and $\angle acd$, where a and b are the middle points between the current tagging line and its neighboring tagging lines in the same image slice at time t, c is the neighboring tagging line which is in the same tagging sheet as the current tagging line at time t, and d is the left hand side tagging lines on the neighboring slice. The deformable mesh is also smoothed with an internal spring force.

Figure 7 shows the results of tracking the tagging sheets. Groups (a) and (b) depict the tracking results of two different tagging sheets. The tag sheet in (a) is located near the RV and the tag sheet in (b) is located near the LV (See Figure 5(b)). The tagging sheets cover the hole heart, from the atria to the ventricle apex. The lower parts of the both tagging sheets are relatively smooth and of big displacement. This is because these two areas correspond to the left ventricle, which is thicker and deforms more than the right ventricles and the atria. From the right hand side portion of the result images in (a) we observe a thin layer whose displacement is relatively big. This corresponds to the right ventricle. Between the right ventricle and the left ventricle we observe the mesh relatively smooth and of small displacement. This is because the tagging sheets are flushed out in the blood pool soon after the systole begins, thus the mesh deforms passively in this region. We also observe relatively irregular meshes in the top portion of both tagging sheets, which is because the atria is very thin and the tagging sheets are not observable. We find visual observation of the two tracking results fits very well with the cardiac anatomy.

V. Conclusions and Future Work

Analysis of the tagged MR images in 3D gives us a concrete framework to incorporate information from the neighboring slices. We have developed a novel 3D Gabor filter bank method to segment and track the 3D tagging sheets over time. In our experiments, some promising tag extraction and tracking results were shown. In future work we will do further analysis based on the Gabor filter parameters. These parameters can be used to extract useful deformation information of the myocardium, such as contraction and twisting. For example, by finding ϕ and ψ that maximizes the Gabor response, we are able to get the orientation of the tagging sheets; by finding the S that maximizes the Gabor response, we can get the spacing between two neighboring tagging sheets. These parameters may let us conduct 3D myocardial strain analysis directly. Accurate estimation of the tagging sheets deformation will also lead to a more dense deformation field which can facilitate the finite element modeling of the heart wall, and ultimately lead to a better understanding of the heart wall motion.

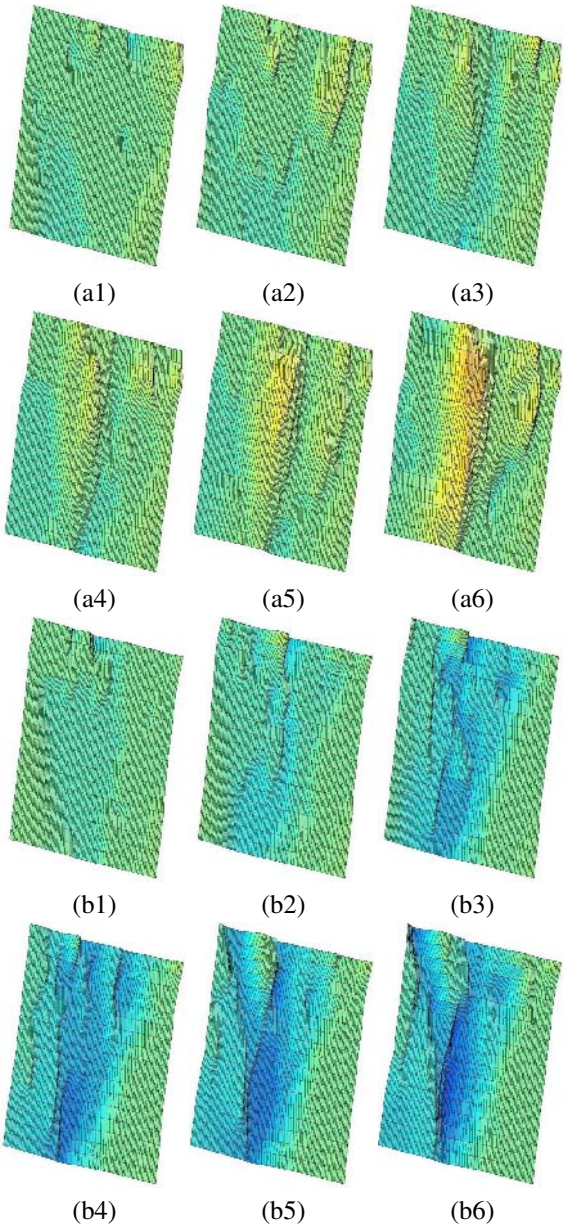

Fig. 7. Tracking results for two tagging sheets at different locations (from time 1 to time 6). The warm color in (a) represents the tagging sheet motion out of the plane and away from the viewer, and the cold color in (b) represents the tagging sheet motion out of the plane and towards the viewer. A deformable mesh is imposed onto each tagging sheet at time 1, and captures the deformation over time.

References

[1] N. F. Osman and J. L. Prince, "Angle images for measuring heart motion from tagged MRI," in *Proc. IEEE Int'l Conf. Image Proc.*, 1998.

[2] N. F. Osman and J. L. Prince, "On the design of the bandpass filters in harmonic phase MRI," in *Proc. IEEE Int'l Conf. Image Proc.*, 2000.

[3] Z. Qian, A. Montillo, D. Metaxas, and L. Axel, "Segmenting cardiac MRI tagging lines using Gabor filter banks," in *Proc of Int'l Conf. of the Engineering in Medicine and Biology Society*, 2003, pp. 630–633.

[4] A. Montillo, L. Axel, and D. Metaxas, "Extracting tissue deformation using Gabor filter banks," in *Proc of SPIE: Medical Imaging: Physiology, Function, and Structure from Medical Images*, 2004, vol. 5369, pp. 1–9.

[5] D. Gabor, "Theory of communication," in *Proceeding of the Institute of Electrical Engineers*, 1946, vol. 93, pp. 429–457.

[6] T. P. Weldon and W. E. Higgins, "An algorithm for designing multiple Gabor filters for segmenting multitextured images," in *IEEE Int'l Conf. on Image Processing*, 1998, vol. 3, pp. 333–337.

[7] M. Fernandez, A. Mavilio, and M. Tejera, "Texture segmentation of a 3D seismic section with wavelet transform and Gabor filters," in *IAPR Int'l Conf. on Pattern Recognition*, 2000, vol. 3, pp. 3358–3361.

[8] A. Madabhushi, M. Feldman, D. Metaxas, D. Chute, and J. Tomaszewski, "A novel stochastic combination of 3D texture features for automated segmentation of prostatic adenocarcinoma from high resolution MRI," in *Medical Imaging Computing and Computer-Assisted Intervention*, 2003, vol. 2, pp. 581–591.

[9] J. Bigun, "Speed, frequency, and orientation tuned 3-D Gabor filter banks and their design," in *IAPR Int'l Conf. on Pattern Recognition*, 1994, vol. c, pp. 184–187.

[10] G. Heidemann, "A neural 3-D object recognition architecture using optimized Gabor filters.," in *IAPR Int'l Conf. on Pattern Recognition*, 1996.